6th semester project
Report

Domain wall and skyrmion dynamics on synthetic antiferromagnet (SAF) for variable tensile stress - a micromagnetic study

Submitted by

Gaurav Kanu
1811067
3rd year Integrated MSc
National Institute of Science Education and Research

Under the guidance of

Dr. Subhankar Bedanta
Associate Professor
National Institute of Science Education and Research

School of Physical Sciences

6th semester project 2021

Contents

Acknowledgment

I take this opportunity to express my deep sincere gratitude to my guide Dr. Subhankar Bedanta(Associate Professor), NISER, Bhubaneswar for his periodic guidance and support during this entire period of the project.

I would also like to sincerely thanks Mr Brindaban Ojha(JRF, NISER), Mr Ashish K Moharana(5th yr Int.MSc, NISER) and Miss Adyashakti Dash(Project student, NISER) for their valuable suggestion and guidance throughout the whole project.

Chapter 1

Introduction

In modern technological devices higher data storage, faster data transfer rate, write speed and read speed has become a necessary need for everyone and each of the latest gadgets in the market comes up with a new technology, however a small change in the nano-sized material can significantly boost or slow the device. In this project an attempt has been made to study the dynamics of topological spin textures on SAF.

A synthetic antiferromagnet (SAF) comprises of 3 layers stacked above each other, where the top and bottom layer are ferromagnetic (FM) and the middle layer (spacer) is non-magnetic. The SAFs are strongly coupled via exchange interactions such as Ruderman–Kittel–Kasuya–Yosid (RKKY) interaction. The SAFs helps us to avoid skyrmion hall effect while studying its dynamics in presence of current in plane (CIP). It also has a very useful application in the manufacture of random access memory (RAM).

The domain walls (DWs) are formed between adjacent domains in magnetic materials, the domain wall motion can be driven by the spin transfer torque (STT), the domain wall (in FM & AFM) applications are increasing as racetrack memories and sensors.

A magnetic skyrmion can be defined as a quasiparticle-like nanometer-scale magnetic DW structure of which the spin configuration is swirling in the planar space and would wrap a unit three-dimensional (3D) spherical surface with spins pointing in all directions in the compactification of the planar space [1].

Whenever a force is applied on an object it leads into deformation of the object while absorbing the impact of the force, such deformations lead

to changes in the geometry of material from nanoscopic level to naked eye distinctions.

In this project work, under the framework of micromagnetics, our main goal is to measure the motion of DW and magnetic skyrmions by applying CIP and under the application of tensile stress which is responsible for the change in the anisotropy of the material thus the ansisotropy constant (K_u).

1.1 Micromagnetism

1.1.1 Ferromagnetic domains

Ferromagnetic domains are small regions in ferromagnetic materials within which all the magnetic dipoles are aligned parallel to each other. When a ferromagnetic material is in its demagnetized state, the magnetization vectors in different domains have different orientations, and the total magnetization averages to zero.

Reason for many domains

In a ferromagnetic material the main reason for occurrence many domains is to reduce the magnetostatic energy, the below diagram depicts how division into smaller domains will help us to reduce the magenetostatic energy.

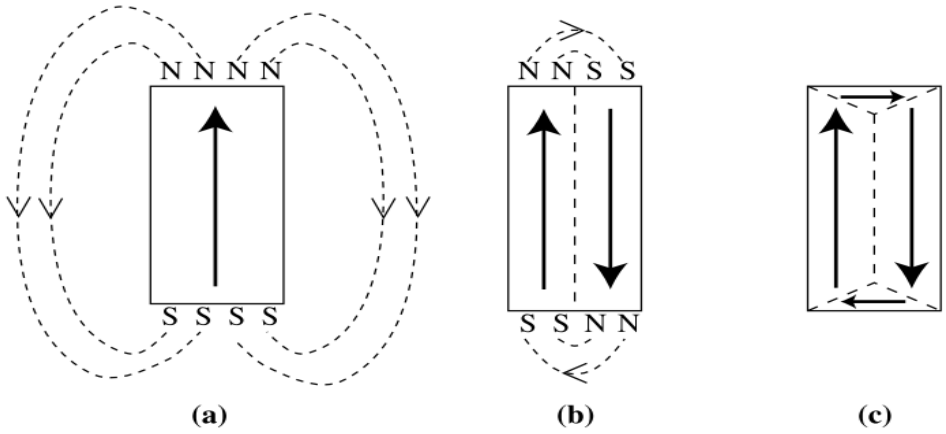

Fig.1: Reduction of the magnetostatic energy by domain formation in a ferromagnet.[2]

1.1.2 Domain walls

Domain walls are the boundaries between the adjacent domains. The adjacent magnetization usually differ by 90°or 180°. There are two types of domain walls: (i) Bloch wall and (ii) Neel wall

Néel and Bloch walls

In Néel wall the rotation of the magnetic moments takes place is in plane whereas in Bloch wall rotation takes place is out of the plane.The Fig.2 shows the rotations in Néel wall and Bloch wall.

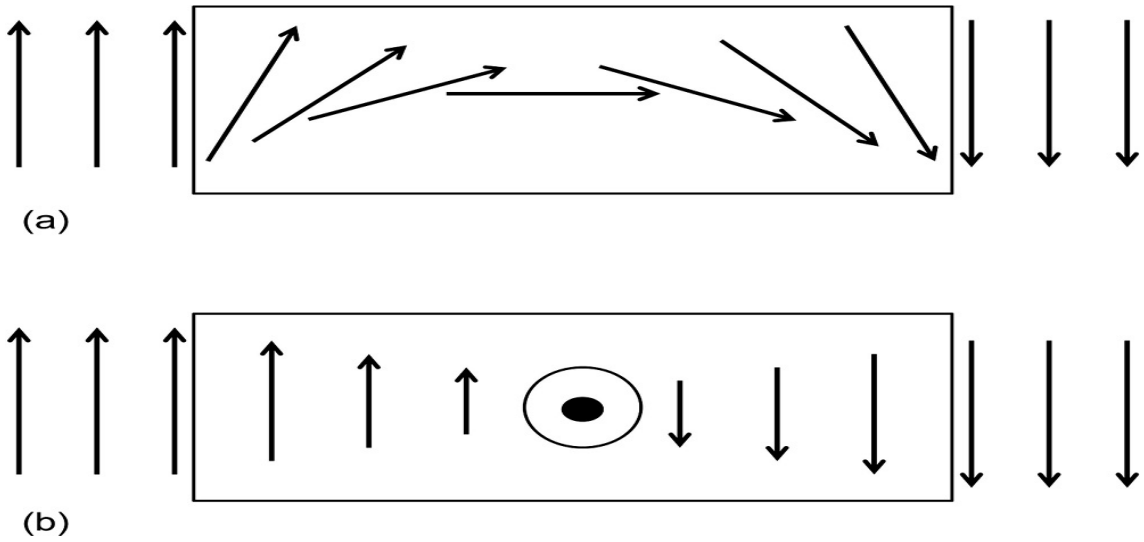

Fig.2: (a) Néel wall and (b) Bloch wall

1.1.3 Magnetic anisotropy

The dependence of the magnetic properties on the direction of the applied field with respect to the crystal lattice. Depending on the orientation of the field with respect to the crystal lattice one would need a lower or higher magnetic field to reach the saturation magnetization. There are several kinds of anisotropy:

- Magnetocrystalline anisotropy- It is intrinsic to the material. It is the energy required to deflect the magnetic moment in a crystal from the easy to the hard direction.

- Shape anisotropy- It is because of the dipolar interaction. This interaction is long range and so its contribution is dependent upon the shape of the sample.
- Stress anisotropy- Change in the anisotropy of the sample because of the strain on the material.
- Exchange anisotropy - Exchange coupling at the interface between two different magnetically ordered systems.

Magnetocrystalline energy

The magnetization in ferromagnetic crystals tends to align along certain preferred crystallographic directions. The preferred directions are called the "easy" axes, since it is easiest to magnetize a demagnetized sample to saturation if the external field is applied along a preferred direction.
Below plot shows the magnetization along easy axes and hard axes.

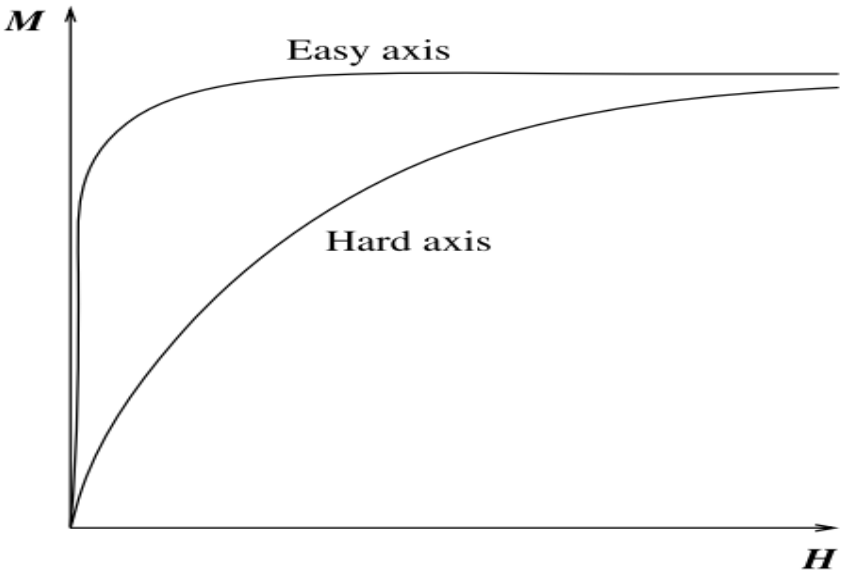

Fig.3: Schematic magnetization curves for a ferromagnet with the field oriented along the hard and easy directions[2].

In both the case saturation magnetization is achieved but much larger applied field is required to reach saturation along the hard axis than along the easy axis.

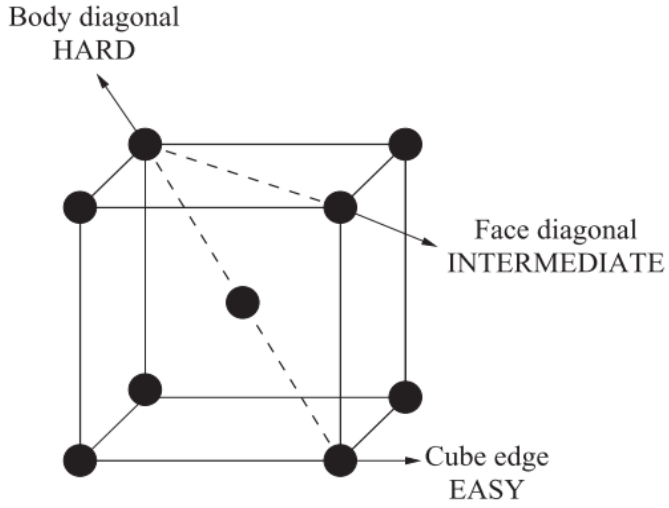

Fig.4: Easy, medium, and hard directions of magnetization in a unit cell of BCC iron.[2]

Cubic crystal:

$$E_a = K_0 + K_1(\alpha_1^2\alpha_2^2 + \alpha_2^2\alpha_3^2 + \alpha_3^2\alpha_1^2) + K_2(\alpha_1^2\alpha_2^2\alpha_3^2) \tag{1.1}$$

$\alpha_1, \alpha_2, \alpha_3$ are the direction cosines, $\alpha_i = \cos\theta_i$ and θ_i are the angles between the magnetization and the easy axes.
K_0, K_1, K_2 are anisotropy constants. For a particular material at a particular temperature and are expressed in erg/cm3 (cgs) or J/m3 (SI).

Uniaxial crystal:

$$E_a = K_u \sin^2\theta \tag{1.2}$$

Where θ is the angle between the magnetization and the easy axis, and K_u are the anisotropy constants. E_a is a minimum when M_s is in that direction. When K_u is positive, energy is minimum at $\theta = 0$ which is the axis of easy magnetization.

1.1.4 Effect of stress on magnetic anisotropy

Magnetostriction is a property of magnetic materials that causes them to change their shape or dimensions during the process of magnetization.

If a material has positive magnetostriction coefficient (λ_l), it will elongate when magnetized.

On imposing an additional strain on the sample it is expected that the direction of the magnetization will change. From our previous knowledge we know that in the absence of strain, the direction of M_s is controlled by crystal anisotropy. Therefore, when a strain is acting, the direction of M_s of the sample is controlled by both strain (σ) and crystal anisotropy. So the general relation which involve both magnetisation (M_s) and stress is given as:

$$E_{me} = \frac{3}{2}\lambda_{si} \sin^2 \theta \tag{1.3}$$

where θ is the angle between Ms and σ.
This relation can show how a material responds to a applied stress depends only by the sign of the product of λ_{si} and σ; of a material.

1.2 Exchange interactions

The interactions among magnetic moments as well as the interactions between magnetic moment and external magnetic field include the Heisenberg exchange interaction, DMI, magnetic anisotropy interaction, Zeeman interaction, and dipole-dipole interaction [1].

1.2.1 Heisenberg exchange

A strong but short-range effect, where only the nearest-neighbor (NN) sites are taken into account usually. According to the Heisenberg exchange model, the energy between neighboring spins, $\mathbf{S_i}$ and $\mathbf{S_j}$ can be written as[1]:

$$\mathbf{H_{Heis}} = -J_{ij} \sum_{i,j} < \mathbf{S_i}.\mathbf{S_j} > \tag{1.4}$$

where $\mathbf{J_{ij}}$ is the exchange constant between $\mathbf{S_i}$ and $\mathbf{S_j}$.

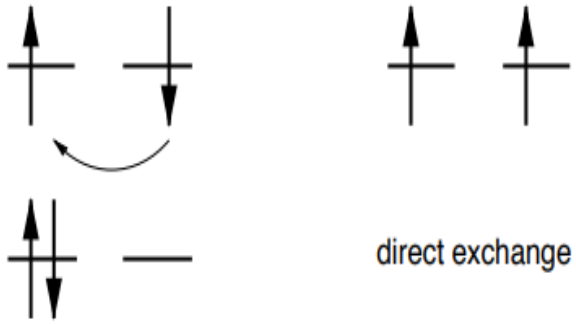

Fig.5: Direct exchange mechanism: The antiparallel alignment of the spins (left) is favored, since it allows the electrons to hop to the neighboring site. For parallel spins (right) hopping is suppressed by the Pauli exclusion principle.

1.2.2 Dzyaloshinskii-Moriya Interaction (DMI):

An antisymmetric exchange interaction, which arises from the spin-orbit coupling [3]. It occurs at the interface between a magnetic thin film layer and a heavy-metal layer with strong spin-orbit coupling and also in the bulk materials lacking inversion symmetry[1].

$$H_{DMI} = (\mathbf{S_1} \times \mathbf{S_2}) . \mathbf{d_{12}} \tag{1.5}$$

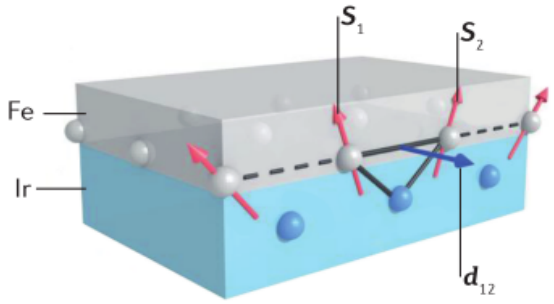

Fig.6: Dzyaloshinskii–Moriya interactions. Schematic picture illustrating the Dzyaloshinskii–Moriya interaction (DMI) at the interface between a magnetic film and a heavy metal. The DMI is mediated by electrons that interact by an exchange mechanism with the spins of the atoms in the magnetic layer, and that have spin–orbit coupling to the heavy metal sites. $\mathbf{S_1}$ and $\mathbf{S_2}$ label the spins of neighbouring atoms, and $\mathbf{d_{12}}$ is the corresponding Dzyaloshinskii–Moriya vector.[4]

1.2.3 Anisotropy:

The energy costs to turn the magnetization from the direction of easy axis into any other direction. In the framework of micromagnetics, the average energy density of the uniaxial magnetic anisotropy is given by[1]:

$$E_{ani} = -\mathbf{K}(\mathbf{m}.\mathbf{n})^2 \tag{1.6}$$

where $\mathbf{K}$ is the anisotropy constant, and $\mathbf{n}$ is the easy axis.

1.2.4 Zeeman energy:

The Zeeman interaction tends to turn the magnetization to the same direction as the applied magnetic field, it is expressed as[1]:

$$E_{Zeeman} = -\mu_0 \int_V (\mathbf{M}.\mathbf{H_{ext}})\, dV \tag{1.7}$$

where $\mathbf{H_{Ext}}$ is the external field, $\mathbf{M}$ the local magnetization and the integral is done over the volume of the body.

1.2.5 Dipole-Dipole interaction

A long-range interaction in which magnetic dipoles generate the demagnetization field $\mathbf{H_d}$, with tendency to act on the moment so as to reduce the total magnetic moment. For the continuous model, the average energy density of the dipole-dipole interaction can be regarded as the Zeeman energy density of the demagnetization field, given as[1]:

$$E_{DDI} = -\frac{\mu_0}{2}(\mathbf{M}.\mathbf{H_{DDI}}) \tag{1.8}$$

where the factor $\frac{1}{2}$ is included to avoid double counting.

1.2.6 Ruderman–Kittel–Kasuya–Yosida (RKKY) interaction

This indirect interaction is the result of the spin polarization of conduction electrons produced by the exchange interaction of the localized moments with conduction electrons where the distance between two localized moments controls the strength of their effective exchange. The oscillatory Ruderman-Kittel-Kasuya-Yosida (RKKY) interaction of the localized magnetic moments in a metal has always played an important role in revealing the nature of the magnetic interaction in metals with partially unfilled d and

f electron shells.[5]

The RKKY interaction which describes the interaction between two local impurity spins at the positions i and j in the form of an XXZ-type effective exchange Hamiltonian[5].

$$\mathcal{H}^{ij}_{\mathrm{RKKY}} = J^{ij}_{x}\left(S^{x}_{i}S^{x}_{j} + S^{y}_{i}S^{y}_{j}\right) + J^{ij}_{z}S^{z}_{i}S^{z}_{j} \tag{1.9}$$

1.3 Magnetic skyrmions

A magnetic skyrmion is a local whirl of the spin conFiguration in a magnetic material. As shown in Fig. 7, the spins inside a skyrmion rotate progressively with a fixed chirality from the up direction at one edge to the down direction at the centre, and then to the up direction again at the other edge[4].
Robust magnetic skyrmions were first experimentally observed in bulk MnSi single crystals that lack inversion symmetry due to its cubic B20 crystal structure[6].

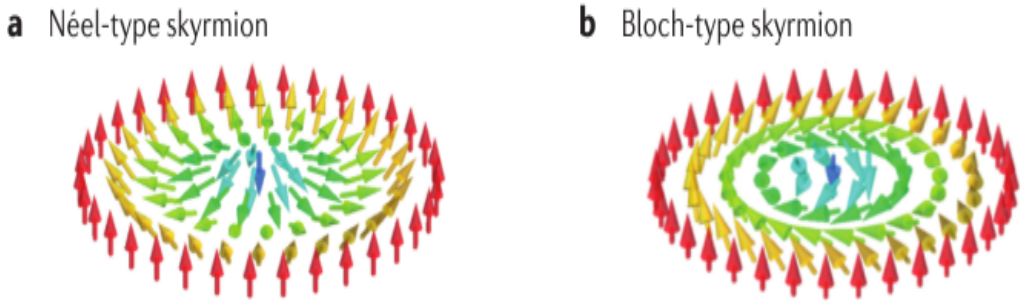

Fig.7: Magnetic texture of skyrmions.— Néel-type(a) and Bloch-type (b) skyrmions with the magnetization rotating from the down direction at the skyrmion's centre to the up direction of the external uniform magnetization at the skyrmion's edge, as in a Néel or in a Bloch domain wall[4].

The up direction spins at the boundaries (in red colour) can be described as north pole as all are facing in the same direction and the spins at the center can be called as south pole (in blue colour) as pointing in opposite direction.

1.3.1 Types of skyrmion:

There are two types of magnetic skyrmions Neel-type and Bloch-type. In Fig. 7. In Neel-type skyrmions the magnetic moments rotate in plane at a particular polar angle, whereas in Bloch-type skyrmion out of plane rotation can be observed.
Any structure will be called a skyrmion if the S (skyrmion number) value is greater than or equal to 1 (i.e +ve integers), discussed more about S in section 1.3.2

1.3.2 Topological number(S)

Magnetic skyrmions stabilization and dynamics depend strongly on their topological properties, the topological number S of magnetic skyrmions is given as:

$$S = \frac{1}{4\pi} \int m \cdot (\partial_x m \times \partial_y m)\, \mathrm{d}x\ \mathrm{d}y = \pm 1 \tag{1.10}$$

where **m** is the normalized local magnetization, the topological number or skyrmion number, is a measure of the winding of the normalized local magnetization.

The non-trivial topology of skyrmion gives rise to the topological protection of the spin conFiguration.

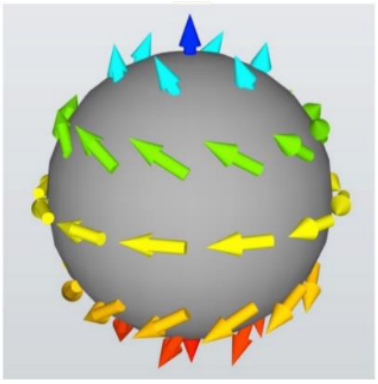

Fig.8: The topological presentation of a magnetic skyrmion by wrapping each individual spin onto a unit sphere[6].

1.3.3 Energy associated with the system

In an ensemble of N atoms on a lattice with lattice constant a. Each atom have a net magnetic moment $\mathbf{m_i} = \mathbf{M_i}/\mathbf{M_s}$, here M_s is the satura-

tion magnetization. The magnetic moment can be defined by atomic spin S_i as $\mathbf{M_i} = \mathbf{g}\mu_\mathbf{B}\mathbf{S_i}$, where g is the gyro-magnetic ratio and μ_B is the Bohr-magneton. The total energy of the assembly of spins in its atomic form is given by:

$$E = E_{ex} + E_{DMI} + E_{aniso} + E_{Zeeman} \tag{1.11}$$

Chapter 2

Simulation details

The Object Oriented Micro-Magnetic Framework (OOMMF) simulation software is a project in the Information Technology Laboratory (ITL) at the National Institute of Standards and Technology (NIST), their goal is to develop a portable, extensible public domain micro-magnetic program and associated tools[7].

Why use OOMMF?

OOMMF is written in C++, a widely-available, object-oriented language that can produce programs with good performance as well as extensibility. For portable user interfaces, Tcl/Tk is used so that OOMMF operates across a wide range of Unix, Windows, and Mac OS X platforms[7].

2.1 Synthetic Anti-ferromagnetic (SAF) Model

Synthetic anti-ferromagnets (SAFs) can be formed by coupling two ferromagnetic (FM) layers with a non-magnetic layer called spacer, as shown in Fig.9. The top and bottom FM layers are coupled anti-ferromagnetically by the RKKY interaction. The bottom FM layer has an isotropic DMI at the interface with lower heavy metal.

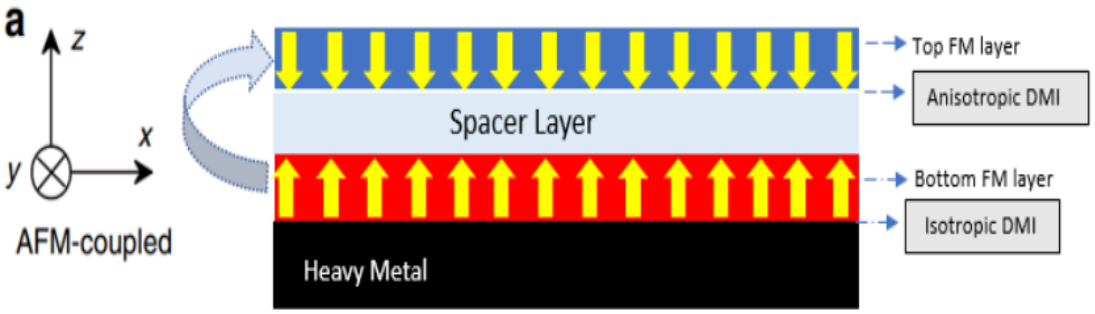

Fig.9: Schematics of the anti-ferromagnetically coupled bilayer thin films.

The Hamiltonian for the system can be given as:

$$\mathrm{H} = -\mathrm{J}_{ex} \sum_{<i,j>} \vec{m}_i \cdot \vec{m}_j + \sum_{<i,j>} D_{iso} \cdot (\vec{m}_{2i} \times \vec{m}_{2j}) + \sum_{<i,j>} D_{\mathrm{Aniso}} \cdot (\vec{m}_{1i} \times \vec{m}_{1j}) - K \sum_i \left(m_i^z\right)^2 + \sigma \left(1 - \vec{m}_{1i} \cdot \vec{m}_{2j}\right) \quad (2.1)$$

where m_i represents the normalized spin at the site i. The first term in equation (2.1) represents the strength of FM interaction between two neighboring spins, where J_{ex} is the FM exchange constant.The second term D_{iso} is the strength of isotropic DMI interaction of spins m_2 between the bottom FM layer and heavy metal. The third term D_{aniso} represents the strength of anisotropic DMI in the top layer of spin m_1. The fourth term provides K the perpendicular magnetic anisotropy (PMA) energy. σ is the strength of RKKY coupling between two layers.The sign of σ is negative for the interlayer AFM interaction. The sigma is given as:

$$\sigma(R) = \frac{m^* k_F^4}{\hbar^2} F\left(2k_F R\right) \quad (2.2)$$

where m is the effective mass and k_F the Fermi wave vector of the electron cloud. The oscillating wave function is given as:

$$F(x) = \frac{xcosx - sinx}{x^4} \quad (2.3)$$

2.2 Landau-Lifshitz-Gilbert (LLG) equation

LLG equation in ferromagnetic material or time evolution of magnetization in a ferromagnetic material is given as:

$$\frac{d\mathbf{M}}{dt} = -\gamma'\mathbf{M} \times \mathbf{H}_{eff} - \lambda\mathbf{M} \times (\mathbf{M} \times \mathbf{H}_{eff}) \tag{2.4}$$

here the terms represents the same physical quantities as described above and $\lambda = \alpha\gamma$, α is the damping constant. Here the first term causes the precession of M around H_{eff} and second term is the damping term[8].

$$\mathbf{H}_{eff} = \mathbf{H}/M_s + \mathbf{H}_{ani} + \mathbf{H}_{ex} \tag{2.5}$$

2.3 Dynamics of domain wall and skyrmionic structure

2.3.1 Spin transfer torque (STT)

In Spintronics, spin transfer torque (STT) play active role to manipulate local magnetization, which are controlled by external magnetic field traditionally.
The STT refers to the effect by spin polarized charge current in magnetic materials when there is magnetization spatial gradient [9]. The advantage of these spin torque effects is that the required current is scalable with magnetization dimension.

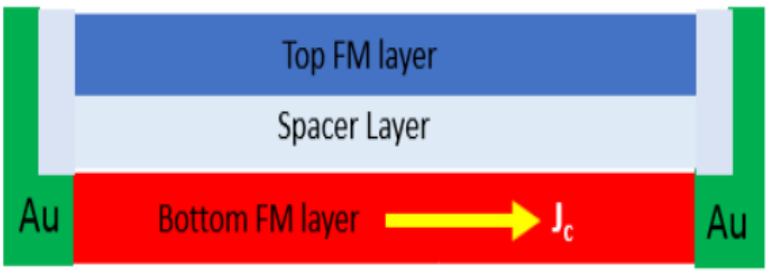

Fig.10: Current in Plane (CIP) responsible for STT, yellow arrow represents the direction of in-plane current in ferromagnetic layer.

From Fig.10 when current is directly applied to the FM layer the conduction electron interacts with the existing magnetization and transfer its spin

angular momentum and this causes in plane torque which can be given by the modified LLG equation:

$$\begin{aligned} \frac{d\vec{M}}{dt} = \gamma_0 \vec{H}_{eff} \times \vec{M} + \frac{\alpha}{M_s}\left(\vec{M} \times \frac{d\vec{M}}{dt}\right) \\ + \frac{u}{M_s^2}\left(\vec{M} \times \frac{\partial \vec{M}}{\partial x} \times \vec{M}\right) - \frac{\beta u}{M_s}\left(\vec{M} \times \frac{\partial \vec{M}}{\partial x}\right) \end{aligned} \tag{2.6}$$

where the 3rd term in the equation is responsible for STT.

Chapter 3

Results and Discussion

3.1 Study of current driven dynamics of SAF domain wall using micro-magnetic simulation

Using the OOMMF software a SAF domain wall is moved by application of current and the respective velocity of the domain wall is measured.

3.1.1 SAF structure

Firstly three stacked layers are created and named as top, spacer and bottom (Fig.11) all are equally sized $1000nm \times 20nm \times 3nm$ (x-y-z).

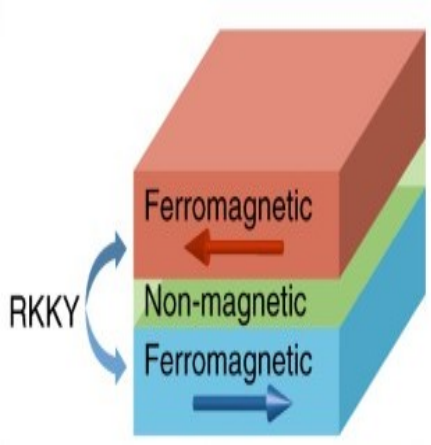

Fig.11: Stacked layers (FM, Spacer, FM) in a SAF

Then a rectangular mesh is created which defines the lattice sites for the atoms, so on defining a periodic location (in our case (5,4,3)nm) the whole lattice sites can be generated.

The layers have a Heisenberg constant as A $= 2 \times 10^{-11} J/m$, DMI exchange as $D = 1.25 mJ/m^2$, saturation magnetization of atom is $M_S = 600 \times 10^3 A/m$, RKKY exchange interaction strength is given by $\sigma = -3 \times 10^{-4}$ and has an initial uniaxial Anisotropy constant $K_1 = 0.3 \times 10^6 J/m^3$.

The applied current in plane (CIP) is given by $u = 500 m/s$ (velocity of electron), for the current density ($\vec{J}$) the expression is given as:

$$u = \frac{JPg\mu_B}{2eM_s} \tag{3.1}$$

where g is the Lande' g factor, μ_B is the Bohr magneton, e is the charge of electron and M_S is the saturation magnetic field.

After adding all the parameters the following domain wall is obtained as shown in the Fig.12:

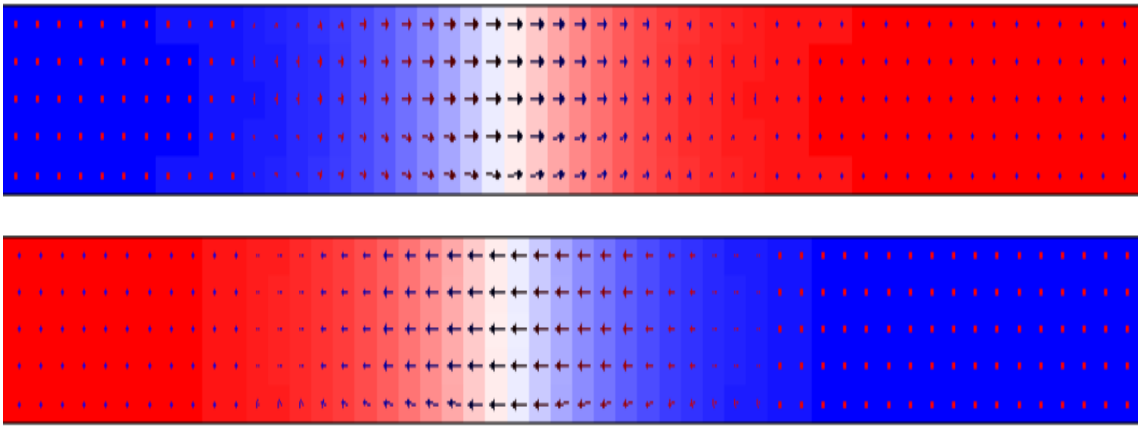

Fig.12: The formation of domain wall on the top and bottom FM layers (1st is the top layer and 2nd is the bottom layer).

In this project we measured the change in the dynamics of domain wall and magnetic skyrmion on SAF on changing the anisotropy constant K_u.

$$\text{Velocity} = \frac{\text{Position}_{\text{final}} - \text{Position}_{\text{initial}}}{\text{Time}_{\text{final}} - \text{Time}_{\text{initial}}} \tag{3.2}$$

The velocity of the domain wall and skymion were calculated via image processing and later the pixels were converted to meter by multiplying by a factor of 2.645833×10^{-4} (i.e. $1px = 2.645833 \times 10^{-4}m$)

3.1.2 Application of tensile stress to the SAF layer

Tensile stress is caused by the pulling forces which causes stretching actions in the material or elongation of the material, the deformation in the material causes change in the geometry of the material that can cause change in the brillouin zone which causes change in the magnetic anisotropy of materials.

In our code we have made changes in the anisotropy constant from $K_u = 0.3 \times 10^6 J/m^3$ to $K_u = 1.2 \times 10^6 J/m^3$ and respectively measured the velocity of DW for each of the K_u values.

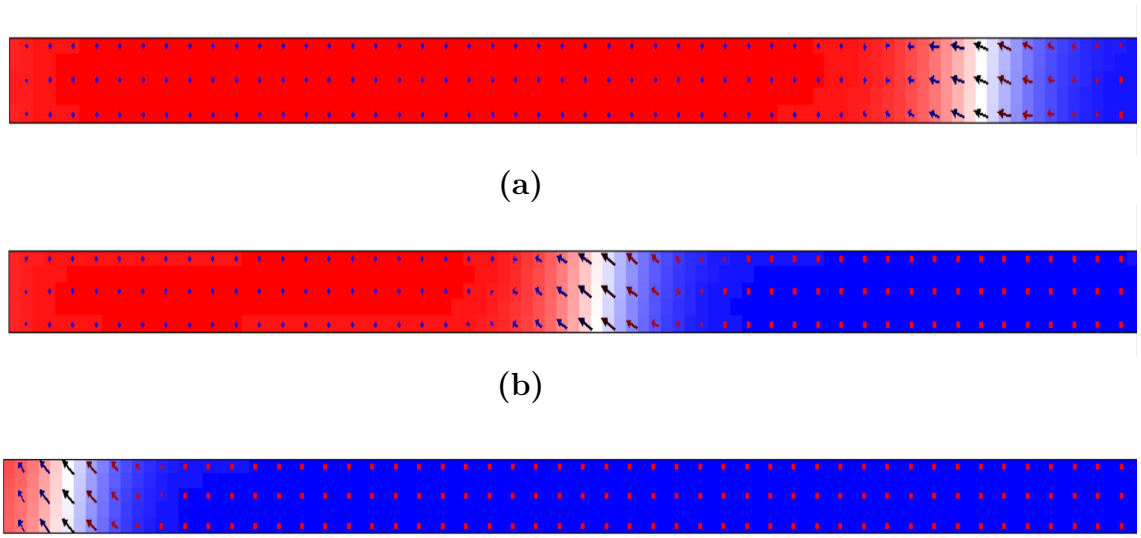

(a)

(b)

(c)

Fig.13: (a-b-c) A moving domain wall (right to left) at $K_u = 0.3 \times 10^6 J/m^3$.

To understand the behaviour of motion of domain wall with the anisotropy of the material Fig.14 - Plot represents velocity vs K_u plot. Under the application of tensile stress in a system, PMA i.e. K_u increases. An increase in K_u results in increasing the DW formation energy. As a result, the DW velocity becomes slower while it propagates in a medium.

Table 3.1: Data values consisting of velocity domain wall at each K_u

Anisotropy (K_u) $\times 10^6 J/m^3$	Velocity (v) m/s
0.3	0.21261
0.4	0.20753
0.5	0.20067
0.6	0.19238
0.7	0.18646
0.8	0.18218
0.9	0.17628
1	0.17018
1.1	0.16574
1.2	0.16022

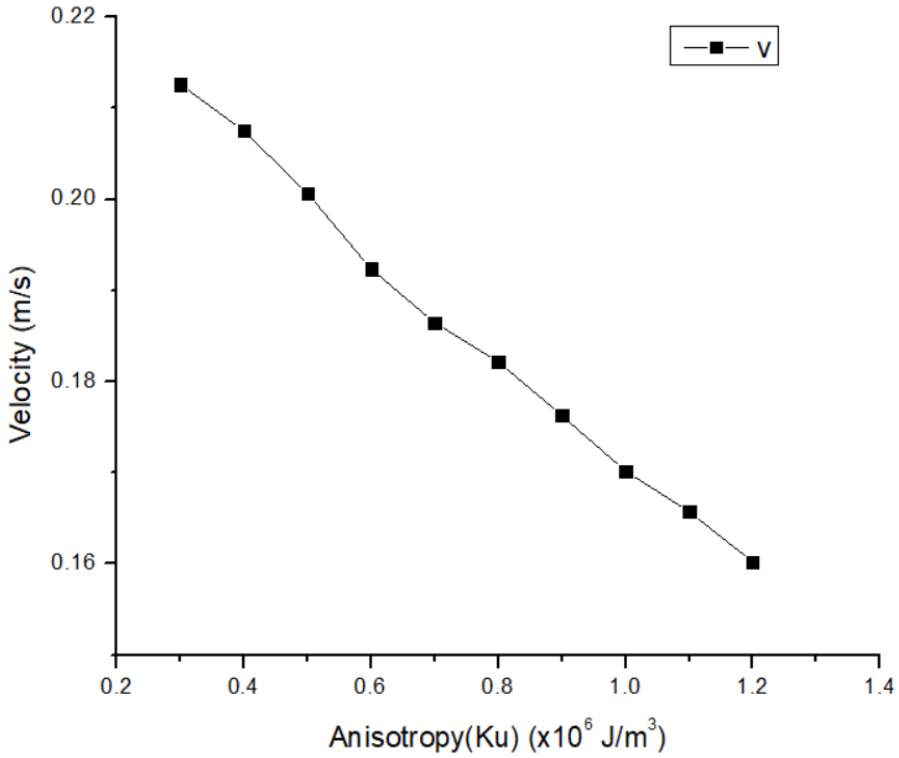

Fig.14: Domain wall velocity vs K_u (anisotropy constant) plot.

From Fig.14 - Plot it is certain that velocity linearly decreases with increase in K_u. Which tells us that application of tensile stress increases the anisotropy in the material which causes decrease in the velocity of domain wall.

3.2 Study of current driven dynamics of SAF magnetic skyrmion using micro-magnetic simulation

3.2.1 SAF structure

Similarly here also firstly three stacked layers are created and named as top, spacer and bottom (Fig.11) all are equally sized $1000nm \times 100nm \times 1nm$ (x-y-z).

Then a rectangular mesh is created which defines the lattice sites for the atoms, so on defining a periodic location (in our case (2,2,1)nm) the whole lattice sites can be generated.

The layers have a Heisenberg constant as A $= 15 \times 10^{-12} J/m$, DMI exchange as $D = 3.4mJ/m^2$, saturation magnetization of atom is $M_S = 580 \times 10^3 A/m$, RKKY exchange interaction strength is given by $\sigma = -2 \times 10^{-3}$ and has an initial uniaxial Anisotropy constant $K_1 = 0.8 \times 10^6 J/m^3$.The applied in plane current is given by $u = 100m/s$

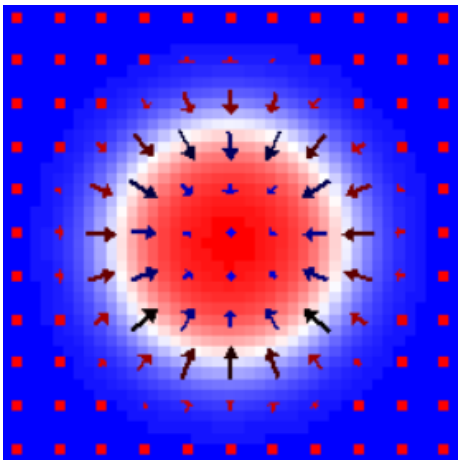

Fig.15: A magnetic skyrmion (OOMMF simulated)

3.2.2 Application of tensile stress to the SAF layer

As discussed earlier in 3.1.2 we know that application of tensile stress will lead to change in anisotropy of the magnetic material. Here the anisotropy constant K_u is changed from $K_u = 0.7 \times 10^6 J/m^3$ to $K_u 1.0 \times 10^6 J/m^3$, and respectively measured the velocity of skyrmion for each of the $K_u$values.

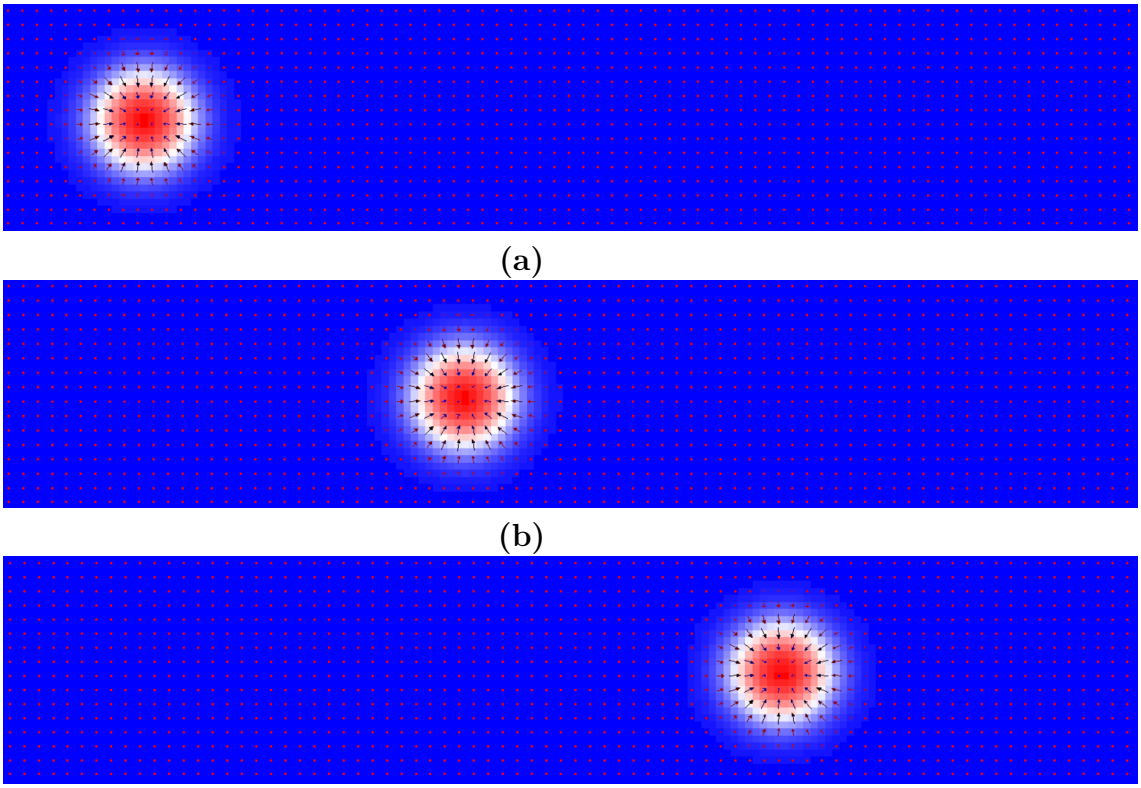

(a)

(b)

(c)

Fig.16: (a-b-c) A moving magnetic skyrmion (left to right) at $K_u = 0.8 \times 10^6 J/m^3$.

Table 3.2: Data values consisting of velocity of magnetic skyrmion at each K_u

Anisotropy (K_u) $\times 10^6 J/m^3$	Velocity (v) m/s
0.7	0.06164
0.75	0.06129
0.8	0.06077
0.85	0.06038
0.9	0.05995
0.95	0.05939
1	0.05892

The plot in Fig.17 represents velocity of magnetic skyrmion at different K_u (anisotropy constant) values :

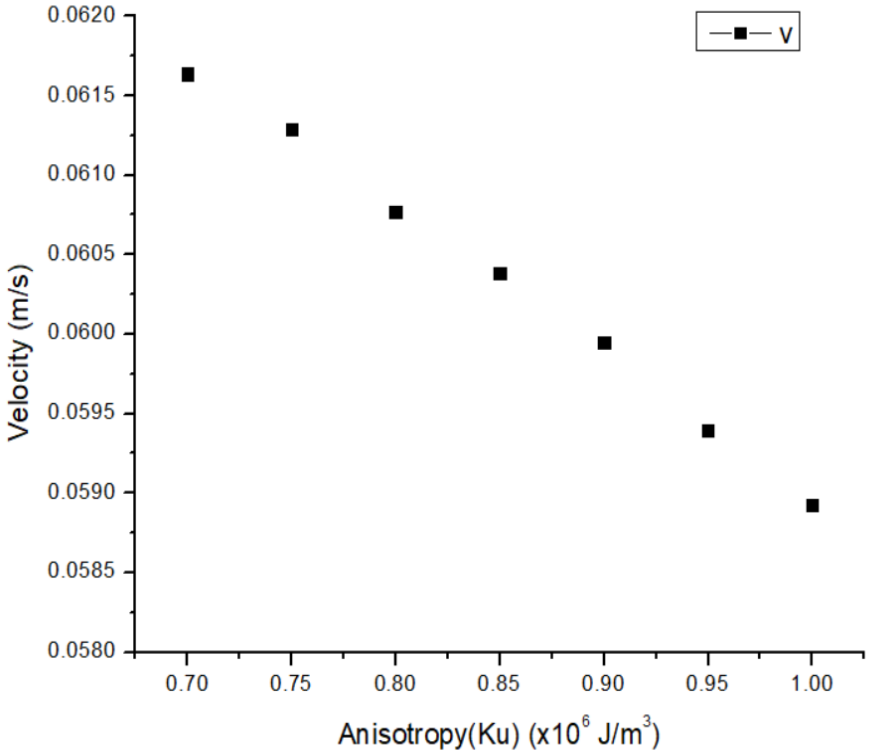

Fig.17: Magnetic skyrmion velocity vs K_u (anisotropy constant) plot.

From the plot in Fig.17 we can infer that as the anisotropy increases the velocity of the skyrmion decreases linearly.

Here we have also observed that the skyrmion velocity decreases with increasing the tensile stress (K_u) as it increases the néel wall formation energy.

The maximum velocity of the domain wall is found to be :

$\tilde{\mathbf{v}} = \mathbf{0.21261m/s}$ for $K_u = 0.3 \times 10^6 J/m^3$ and $\vec{J} = 1.17778 \times 10^{13} A/m^2$

Similarly the maximum velocity of the magnetic skyrmion is found to be:

$\tilde{\mathbf{v}} = \mathbf{0.06164m/s}$ for $K_u = 0.7 \times 10^6 J/m^3$ and $\vec{J} = 2.277 \times 10^{12} A/m^2$

Chapter 4

Conclusion

In this project we have stabilized DW and skyrmion in SAF structure. We have studied the DW and skyrmion dynamics by varying tensile stress. Due to the tensile stress the PMA has increased in our system and a significant effect of stress has been observed. The velocity of both domain wall and skyrmion got reduced with increasing the tensile stress (PMA).

The velocity of the DW is nearly 3.5 times higher than skyrmion in a SAF system.

References

[1] X. Zhang, "Dynamics of magnetic skyrmions in nanostructures and their applications." `https://soar-ir.repo.nii.ac.jp/record/20148/files/18TR0001_ronbun.pdf`, 2018.

[2] N. A. Spaldin, *Magnetic Materials: Fundamentals and Applications*. Cambridge University Press, 2 ed., 2010.

[3] T. Moriya, "Anisotropic superexchange interaction and weak ferromagnetism," *Physical review*, vol. 120, no. 1, p. 91, 1960.

[4] A. Fert, N. Reyren, and V. Cros, "Magnetic skyrmions: advances in physics and potential applications," *Nature Reviews Materials*, vol. 2, no. 7, pp. 1–15, 2017.

[5] A. Akbari, I. Eremin, and P. Thalmeier, "Rkky interaction in the spin-density-wave phase of iron-based superconductors," *Physical Review B*, vol. 84, no. 13, p. 134513, 2011.

[6] W. Jiang, G. Chen, K. Liu, J. Zang, S. G. Te Velthuis, and A. Hoffmann, "Skyrmions in magnetic multilayers," *Physics Reports*, vol. 704, pp. 1–49, 2017.

[7] M. J. Donahue and D. G. Porter, "Oommf user's guide, version 1.0." `http://math.nist.gov/oommf`, Sept 1999.

[8] M. Lakshmanan, "The fascinating world of the landau–lifshitz–gilbert equation: an overview," *Philosophical Transactions of the Royal Society A: Mathematical, Physical and Engineering Sciences*, vol. 369, no. 1939, pp. 1280–1300, 2011.

[9] S.-F. Lee, "Spin transfer torque, spin orbit torque and pure spin current,"